

Melting of Poly(oxyethylene) Analyzed by Temperature-Modulated Calorimetry

Kazuhiko Ishikiriya[†] and Bernhard Wunderlich*

Department of Chemistry, University of Tennessee, Knoxville, Tennessee 37996-1600, and Chemistry and Analytical Sciences Division, Oak Ridge National Laboratory, Oak Ridge, Tennessee 37831-6197

Received December 6, 1996[⊗]

ABSTRACT: Recently a small amount of locally reversible melting was observed in semicrystalline poly(ethylene terephthalate) during temperature-modulated differential scanning calorimetry (TMDSC). To further study the reversibility of melting, poly(oxyethylene) (POE) is analyzed. Low molar mass POE is known to be able to form extended-chain, equilibrium crystals, while at higher molar mass and less favorable crystallization conditions, nonequilibrium, folded-chain crystals grow. The TMDSC of POE reveals variable amounts of reversible melting depending on crystallization conditions and molar mass. The crystals closest to equilibrium show no reversible melting, proving the inherently irreversible nature of polymer melting. Crystals of high molar mass show a small amount of the prior discovered locally reversible melting. Poorly crystallized POE of low molar mass have, because of their lower zero-entropy-production melting temperature, a sufficiently smaller gap between crystallization and melting temperature to show some reversing melting.

Introduction

Melting and crystallization of flexible macromolecules present a special problem since the sequence of repeating units must be maintained during the phase transition and the overall conformation of the molecule, the macroconformation, must undergo a drastic rearrangement.¹ In fact, the structure of flexible molecules in the melt has been called *anticrystalline* because of conformational isomerization introduced on melting.² Crystals of rigid and spherical motifs, in contrast, lead on melting to a *quasi-crystalline* structure that can be related to the crystal structure and its lattice.

First observations of temperature-modulated calorimetry (TMC) offered support to the suggestion that there exists reversibility of polymer melting, but only on a molecular or submolecular scale.^{3,4} As soon as a molecule is completely melted, reversibility is lost due to the need of *molecular nucleation*, a rate-determining step with a free-enthalpy barrier for the beginning of crystallization of a molecule, or, at higher supercooling, part of a molecule on the surface of a crystal.^{5–7} Before melting of a molecule is complete, i.e., a part larger or equal to a molecular nucleus remains crystallized, melting and crystallization were shown to be locally reversible within a fraction of a kelvin.⁴ Crystal nucleation is the first step of any crystallization,¹ but it can easily be avoided on addition of external nuclei or by incomplete melting before crystallization (self-nucleation⁸). Molecular nucleation, in contrast, can only be affected by changing the molecular conformation in the melt or solution (e.g., crystallization under conditions of extensive flow⁹).

The studies of this paper are based on temperature-modulated differential scanning calorimetry (TMDSC), a new thermal analysis technique.^{10–12} Specifically, a calorimeter of the heat-flux type, the modulated DSC of TA Instruments (MDSC), was used to study the melting region of a series of poly(oxyethylene)s (POE) of different molar mass, so that crystals of different fold-

morphology could be produced.^{13–15} The temperature modulation was done quasi-isothermally,¹⁶ i.e., at constant base temperatures T_0 . This is different from normal TMDSC which superimposes the temperature modulation on an underlying heating rate $\langle q \rangle$. In the present experiments $\langle q \rangle = 0$, and the melting region is traversed with a series of separate, quasi-isothermal runs at constant values of T_0 that are increased or decreased by 2–5 K from one run to the next. The results are also compared to standard, not modulated, DSC with a constant heating rate $dT/dt = q = 10$ K/min. At steady state, the sample temperature in a quasi-isothermal run, $T_s(t)$, is given by:

$$T_s(t) = T_0 + A \sin(\omega t - \epsilon) \quad (1)$$

where A is the maximum amplitude of the sample-temperature oscillation of, usually, 0.5 K; ω , the angular modulation frequency $2\pi/p$, with p being the modulation period of 60 s; and ϵ , the phase shift relative to a reference oscillation. An analogous equation holds for the reference temperature, T_r (maximum amplitude A_r and phase shift ϕ). The reference calorimeter consists of an empty aluminum pan. The temperature difference, $\Delta T = T_r - T_s$ (maximum amplitude A_Δ and phase shift δ) is then proportional to the heat flow (HF) and is used as a response function for the computation of the heat capacity. The modulation amplitude of the block temperature is regulated such that the sample-temperature amplitude, A , achieves the value chosen for the experiment. A full description of the method was given earlier.^{16,17} Analysis of the data relies on achievement of steady state.¹⁸ The quasi-isothermal method allows extended-time experiments, so that one can separate irreversible crystal rearrangements, annealing, and recrystallization processes from the reversible heat capacity, melting, and crystallization.

The heat flow caused by the temperature modulation measures the “reversing” heat capacity, a term introduced in TMDSC to identify a heat effect that can be reversed within the temperature range of the modulation amplitude. To determine if this effect is thermodynamically reversible, the free enthalpy and entropy need be established. As long as the heat capacity

[†] On leave from Toray Research Center, Inc., Otsu, Shiga 520, Japan.

[⊗] Abstract published in *Advance ACS Abstracts*, July 1, 1997.

contribution is fast, the reversing heat capacity is, indeed, the reversible, equilibrium effect. If slow processes or transitions are involved, the reversing heat capacity is an "apparent" heat capacity and in need of special interpretation. The reversing heat capacity as calculated by the MDSC software is the first harmonic response to the modulation with frequency ω of the temperature difference, A_Δ , using a partial Fourier analysis:¹⁷

$$m_{c_p} = \frac{A_\Delta}{A} \sqrt{\left(\frac{K}{\omega}\right)^2 + C^2} = \frac{A_{HF}}{A} K' \quad (2)$$

where A and ω are parameters set at the beginning of the experiment, and C is the heat capacity of the empty reference pan. The Newton's law calibration constant K is independent of modulation frequency and reference heat capacity. The "total heat capacity," consisting of reversing and nonreversing contributions, either can be determined from a standard DSC measurement or extracted from normal TMDSC with an underlying heating rate $\langle q \rangle$:

$$m_{c_p} \approx \frac{K \langle \Delta T \rangle}{\langle q \rangle} = \frac{K' \langle HF \rangle}{\langle q \rangle} \quad (3)$$

For standard DSC, the values in angular brackets are the measured ΔT and chosen values of q ; in TMDSC they are the appropriate sliding averages over full modulation periods ($\pm 1/2p$). This averaging eliminates the modulation effect of the first and higher harmonics of ω . In case the heat capacity is reversible, eqs 2 and 3 give the same results. If not, the reversing heat capacity may still give the equilibrium heat capacity, unless reversing transition effects distort the sinusoidal response to the modulation and cause higher harmonics that would have to be evaluated directly from the instantaneous response (in the time domain) or from a full Fourier series fit. In the present quasi-isothermal experiments $\langle q \rangle = 0$, so that the total heat capacity is not available but is deduced from the separate, standard DSC experiments. Also, the "nonreversing" heat capacity, obtained by calculating the difference between the total and reversing heat capacity, is not available from quasi-isothermal experiments.

Many first-order melting and disordering transitions are sufficiently fast, so that their kinetics can be neglected.¹ For transitions with low enthalpy changes over a wider temperature range it may be possible to keep steady state during melting. Then, the transition can be extracted from the "apparent heat capacity" by subtracting the appropriate baseline of the known, transition-free heat capacity which is available, for example, from the ATHAS Data Bank.¹⁹ For sufficiently small apparent heat capacities, steady state may even be reached in TMDSC.

A quite different behavior is often observed for semicrystalline polymers. During melting they may recrystallize, anneal, and perfect. These processes occur via nonequilibrium paths.¹ If these processes are far from equilibrium or sufficiently fast, they may not be modulated and are observed as fully irreversible phenomena in TMDSC; i.e., they show only in the total heat flow of eq 3 and give no contribution to the reversing heat capacity of eq 2.^{10–12} For the case that the heating cycle of TMDSC can achieve melting under zero-entropy-production conditions²⁰ and the supercooling of the just melted polymer needed for crystallization is more than twice the modulation amplitude ($2A$), one would expect

an endotherm during the first positive modulation that exceeds the melting temperature, not to be followed by a corresponding crystallization exotherm on cooling. In quasi-isothermal experiments any initial loss of steady state due to excessive heat of fusion would die down after a few cycles. As a result, one expects, after the initial melting, a response solely due to the heat capacity given by eq 2 for the fully or partially melted sample. If one finds additional contributions to give a higher apparent heat capacity, these must originate from reversing melting and crystallization.

Experimental Details

Instrumentation, Calibration, and Measurements. A commercial temperature-modulated DSC (TMDSC) of the type Thermal Analyst 2920 MDSC from TA Instruments Inc. was used for the measurements. Cooling was accomplished with a refrigerated cooling system (RCS; cooling capacity to 220 K). Dry nitrogen gas with a flow rate of 20 mL min⁻¹ was purged through the MDSC cell. In order to minimize the loss of steady state during melting, the sample mass was only about 1.0 mg for both the DSC runs (without modulation, heating rate 10 K min⁻¹) and the quasi-isothermal TMDSC runs ($p = 60$ s, $A = 0.5$ K, no underlying heating rates $\langle q \rangle = 0$, separate runs for different values of T_0 ; see eq 1).

For the calibration of the heat-flow amplitudes, 20.2 mg of sapphire was used in parallel experiments of the DSC and quasi-isothermal TMDSC runs to eliminate K , K' , or K'' from eqs 3 and 2, respectively.²¹ The asymmetry correction for the MDSC amplitudes was accomplished by introduction of a fixed cell imbalance, caused by a reference pan of 21 mg and sample pans of close to 23 mg. In this configuration of the calorimeters, the sign of the asymmetry is always positive, and errors of background subtraction due to the unknown sign of the result of eq 2 can be avoided.²² The three runs for quantitative measurements were: one with POE vs empty reference pan, one with sapphire vs empty reference pan, and one with two empty pans. All three runs were made with pans of the same weights and imbalance.

The temperature of the TMDSC equipment was initially calibrated in the standard DSC mode by using the onsets of the melting-transition peaks for water (273.15 K), indium (429.75 K), and tin (505.08 K) at a scanning rate of 10 K min⁻¹. Then, the temperatures in the quasi-isothermal experiments were calibrated using a method developed by the authors.²³ The melting temperature of indium was established under quasi-isothermal conditions with a modulation amplitude of only ± 0.05 K in steps of 0.1 K ($p = 60$ s) and compared to the conditions of the larger amplitude for determination of the temperature correction. In the present case the correction was +0.4 K, which was added to the indicated value.

The major experiments were carried out quasi-isothermally. Separate runs were carried out over the temperature range of 220–370 K with a stepwise temperature increase from 2–5 K, depending on the change in heat capacity in the temperature range. Each quasi-isothermal run lasted 20 min. The heat capacity data of the last 10 min, or for temperatures of slow approach to steady state within 1% deviation from the last point, were averaged and taken as the data point for the given T_0 . Under the chosen measurement conditions the TMDSC software deconvolutes 200 data points over a 10 min time interval for the average maximum heat-flow amplitude. A modeling scheme of the deconvolution has been presented earlier.²⁴

The crystallinity of POE was determined from the enthalpy of fusion measured with conventional DSC on heating at 10 K min⁻¹. The DSC melting peak area was calibrated, as usual, with the heat of fusion of indium.

Sample Description. Three poly(oxyethylene)s (POE) of different molar mass were purchased from Polyscience, Inc. The POEs had the following characteristics: POE1500, catalog number 15647, molar mass standard for 1500 Da, and $M_w/M_n = 1.10$; POE5000, catalog number 15648, molar mass standard for 4540 Da, and $M_w/M_n = 1.05$; POE35,000, catalog number

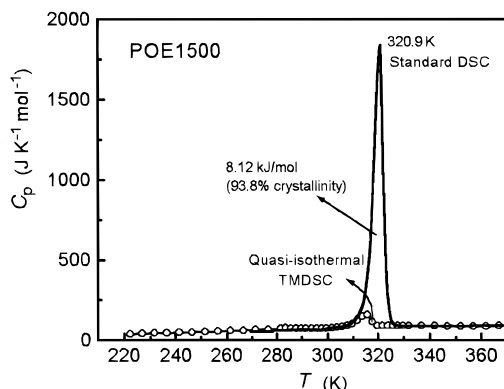


Figure 1. Heat capacity measured by DSC and TMDSC for POE1500 crystallized at 300 K. The solid curve was obtained by DSC at 10 K min^{-1} , and the open circles represent the reversing heat capacity, obtained by quasi-isothermal experiments.

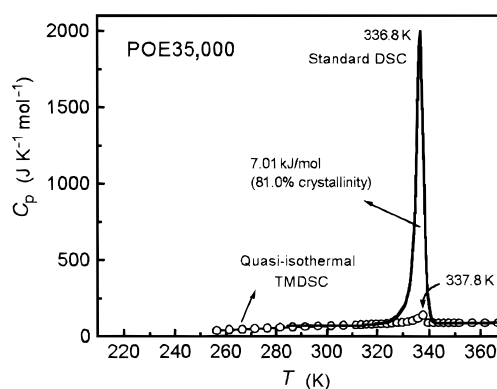


Figure 3. Heat capacity measured by DSC and TMDSC for POE35,000 crystallized on cooling from the melt at 10 K min^{-1} . The solid curve was obtained by DSC at 10 K min^{-1} , and the open circles represent the reversing heat capacity, obtained by quasi-isothermal experiments.

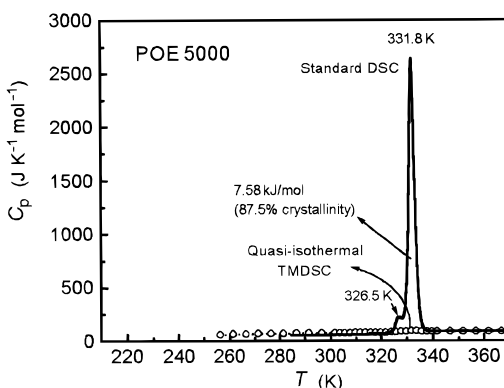


Figure 2. Heat capacity measured by DSC and TMDSC for POE5000 crystallized at 320 K. The solid curve was obtained by DSC at 10 K min^{-1} , and the open circles represent the reversing heat capacity, obtained by quasi-isothermal experiments.

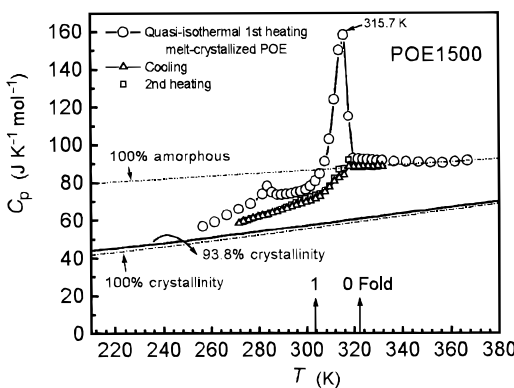


Figure 4. Quasi-isothermal TMDSC of POE1500 on heating and cooling. Circles, triangles, and squares represent the first heating sequence (as in Figure 1), a subsequent cooling sequence, and a second heating sequence, respectively. Indicated also are data bank heat capacities.

22569, molar mass 35 000 Da of broader molar mass distribution. Melt-crystallized samples were used for DSC and TMDSC measurements. Both POE1500 and POE5000 were kept at 383 K for 10 min and then crystallized at 300 K for 10 min and 320 K for 30 min, respectively. For POE1500 this crystallization is complete within about 1 min; i.e., it leads to rather poor crystals. For POE5000 the crystallization was complete in about 20 min and leads to better crystals. The POE35,000 was crystallized by continuous cooling from the melt at 10 K min^{-1} to produce a typical, semicrystalline polymer.

Results

Figure 1 shows the result of the first heating of the melt-crystallized POE1500. Besides the quasi-isothermal TMDSC data (open circles), the total heat capacity is plotted as determined by standard DSC (heavy solid line). The peak temperature of the standard DSC trace is close to the equilibrium melting temperature of extended-chain crystals ($T_m^\circ = 322.3\text{ K}^{15}$). The quasi-isothermal heat capacity shows only a very small indication of a reversing contribution of melting on the low-temperature side of the melting peak.

The results for the melt-crystallized POE5000 are shown in Figure 2. The standard DSC trace shows a small annealing peak at 326.5 K. The quasi-isothermal experiments show practically no reversing melting and crystallization. This occurs despite lower crystallinity than sample POE1500 and a lower than equilibrium melting peak temperature ($T_m^\circ = 333.8\text{ K}^{15}$).

The data for the higher molar mass POE35,000, crystallized on continuous cooling from the melt, are shown in Figure 3. The peak temperature of the DSC trace corresponds to melting of a crystal with 4 folds/molecule (336.8 K^{15}). A peak in the reversible heat capacity can be seen but is, in contrast to the POE1500, on the high-temperature side of the melting peak.

The study of the reversing melting of POE1500 and POE5000 was extended by proceeding with the quasi-isothermal TMDSC after initial melting by stepwise cooling and renewed stepwise heating for a second melting sequence. Figure 4 shows the data for POE1500. The heat capacity scale is expanded relative to Figure 1. Data bank values¹⁹ for the heat capacity of 100% crystallinity and melt (100% amorphous), as well as the semicrystalline POE, are also indicated in Figure 4. Because of the small sample size, an internal calibration was made with the experimental heat capacity of the melt. The small peak in heat capacity on first heating (circles), visible in Figure 1, is located in-between the melting temperatures of crystals with 0 and 1 fold/molecule.¹⁵ A second, minor maximum occurs at about 280 K. The subsequent quasi-isothermal steps on cooling (triangles) and second heating (squares) show only the approach of the heat capacity to the value of the melt without any reversing contribution from the crystallization/melting transition.

Figure 5 displays the data for POE5000. On first heating (circles), a very small reversing melting peak appears at 285 K and a not much larger second one at

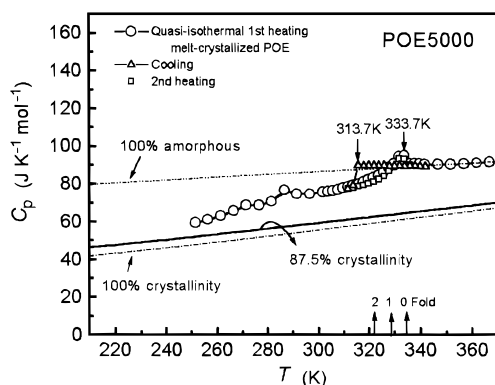


Figure 5. Quasi-isothermal TMDSC of POE5000 on heating and cooling. Circles, triangles, and squares represent the first heating sequence (as in Figure 2), a subsequent cooling sequence, and a second heating sequence, respectively. Indicated also are data bank heat capacities.

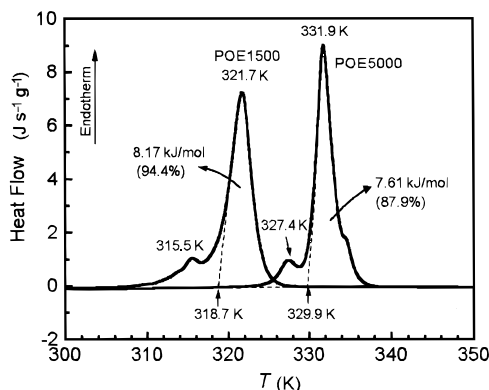


Figure 6. DSC heating curves of POE1500 and POE5000 after the quasi-isothermal cooling sequences of Figures 4 and 5.

333.7 K. Both are not visible in the smaller scale of Figure 2. On cooling (triangles), a supercooling of about 20 K, to 313.7 K, takes place before the heat capacity decreases due to crystallization. No peak can be detected for a reversible heat capacity contribution due to melting/crystallization. On second heating (squares), a very small peak appears at 333.7 K, the same temperature as on first heating.

To check on the nature of the crystals that were produced on the cooling runs, standard DSC measurements were made on similarly produced samples of POE1500 and POE5000. Figure 6 shows the results. The melting curves indicate improvements in crystal perfection, particularly for POE1500.

Finally, in Figure 7, it is shown that at the peak temperature of Figure 1 it takes a long time to approach steady state. The quasi-isothermal, reversing, apparent heat capacity of POE1500 slowly reaches a *higher* level than initially observed (compare to Figure 1, data after 20 min). This observation is in contrast to changes to *lower* levels that were observed in the analysis of poly(ethylene terephthalate) (PET).⁴ The PET data were explained by a slow loss of partially crystallized molecules that could reversibly melt and crystallize. For POE5000 the reversing increase in heat capacity is too small to clearly identify decreases or increases at longer times. POE35,000 shows only the "normal" decrease of the apparent heat capacity with time in the melting range, as seen in PET.⁴ The change in crystallinity listed in Figure 7 was assessed by repeat experiments, stopped at the indicated times and continued by standard DSC for evaluation of the melting peak. The

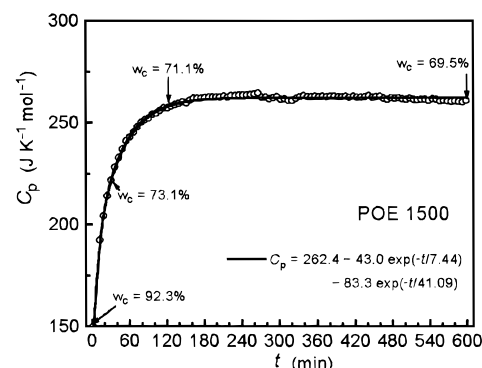


Figure 7. Change of the apparent heat capacity at 315.7 K of POE1500 as a function of time (temperature close to the maximum in apparent reversing heat capacity, sample of Figure 1; see also Figure 4, open circles).

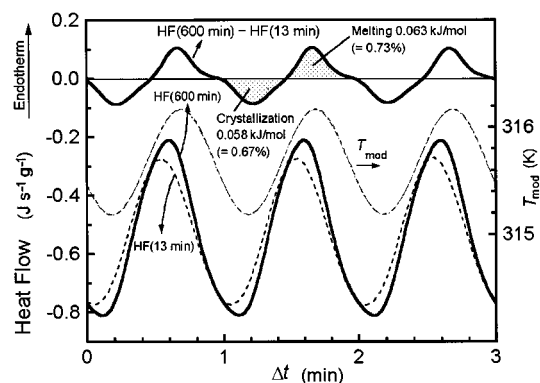


Figure 8. Excerpts of the heat flows as a function of time at 315.7 K ending at 13 and 600 min of the experiment of Figure 7. Also shown are the differences between the two heat-flow curves and the modulated temperature.

largest decrease in crystallinity occurs within the first few minutes on increasing the temperature to the chosen T_0 (decrease by about 19%). The drawn-out exponential curve in Figure 7 is fitted to the measured points.

A comparison of the heat-flow curves of the experiment of Figure 7 in the time domain at about 13 and 600 min is shown in Figure 8. The instantaneous heat flows $HF(t)$ approaching 13 and 600 min are plotted at the bottom of the figure. A subtraction of the two curves is given in the upper trace. The modulated temperature is the curve in the middle, given for reference. The larger exothermic and endothermic signals at later time are seen in each cycle. Added latent heats of melting and crystallization cause the increase in the apparent heat capacity. For the difference curve, the latent heats have been estimated. They yield a change of about 0.7% in crystallinity. Note also that melting and crystallization occur at different temperatures and that the heat-flow curve is not strictly sinusoidal, so that the first harmonic Fourier component used for the computation of the reversing heat capacity of eq 2 does not contain the full heats of transition.

Finally, Figure 9 shows the Lissajous figures of a plot of instantaneous heat flow vs temperature at different times of the long-time experiment of Figure 7. It shows the slow shift in $HF(t)$ at constant modulation at 315.7 K and proves that steady state was maintained between 13 and 600 min.

Discussion

It is by now well-known that TMDSC can separate irreversible effects from the reversing heat capacity

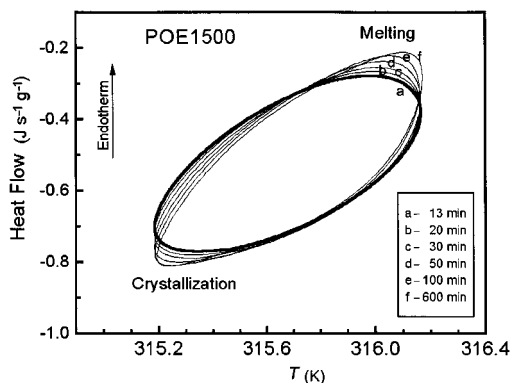


Figure 9. Lissajous figures of heat flow vs temperature at 13, 20, 30, 50, 100, and 600 min under quasi-isothermal conditions at 315.7 K with a temperature amplitude of ± 0.5 K (data of Figure 7).

contributions.^{10–12} The apparent, time-dependent heat capacities of poly(ethylene terephthalate) and polystyrene in the glass transition region could be analyzed quantitatively by separation from the nonreversing enthalpy relaxation.^{25,26} The progress of curing of epoxies was checked by measurement of the reversing heat capacity in the glass transition region in the presence of an irreversible heat of reaction.²⁷ The kinetics of crystallization of polyethylene could be evaluated using the change in heat capacity in the presence of the irreversible heat of crystallization.²⁸ The present analyses of POE1500 and POE5000 in Figures 4 and 5 show that melting is practically completely irreversible for sufficiently well-crystallized, long-chain molecules. The major melting range of the molecules can be judged to be 2–3 K wide when comparing the separation of the extrapolated onset of melting from the melting peak (see Figure 6). This temperature range is several times the modulation width (± 0.5 K); i.e., in the melting range, crystal nuclei remain during the cooling cycle but do not initiate recrystallization of any of the melted molecules. The quasi-isothermal analysis of the melting of POE can, thus, be taken as proof that *molecular nucleation* is needed in addition to crystal nucleation. Molecular nucleation was discovered earlier when it became necessary to explain molecular mass separations below the equilibrium melting temperature^{5–7} and the inability to enhance crystallization by nucleation with extended-chain, equilibrium crystals.²⁹ Quite in contrast to the melting of macromolecules, quasi-isothermal experiments with indium show reversible melting and crystallization as long as the melting during the heating cycle is incomplete and nuclei are left for crystallization.²³ Since indium melts rather sharply, these experiments had to be performed with a small modulation amplitude of 0.05 K and had to rely on insufficient heat flow for incomplete melting during the heating cycle.

The minor maximum in the apparent, reversing heat capacity of the less well-crystallized POE1500 and the true macromolecules of POE35,000 seen in Figures 1 and 3 allows some additional insight into the melting and crystallization mechanisms of macromolecules. In comparison to the DSC melting peak, the amount of reversing melting is small. It is also less than the locally reversible melting observed in the earlier analyzed melt-crystallized PET.^{3,4} While POE35,000 behaves similar to PET, the apparent heat capacity of POE1500 on initial heating is different. The position of the peak in the apparent, reversing heat capacity of

POE1500 of Figure 1 is at the low-temperature side of the melting peak and that of POE35,000 of Figure 3 and PET is on the high-temperature side (for PET see Figure 6 of ref 4). For polyethylene, it was proven earlier that a fraction of molecules attached to higher melting crystals could not be extracted with solvents after partial melting and was found to participate only in the high-temperature end of the melting peak.³¹ Such tie molecules between crystals were suggested to be necessary for the locally reversible recrystallization of PET⁴ and are assumed to occur also in POE35,000. Furthermore, the apparent heat capacity of POE1500 increases with time, as shown in Figure 7, while that of POE35,000 and PET decreases (for PET see Figure 3 of ref 3). For PET and POE35,000 the decrease in reversing heat capacity with time is interpreted as a loss of restraint of the molecules with time due to crystal perfection. Figure 7 shows that the reversing heat capacity of POE1500 increases with time and reaches a steady state. Both differences of POE1500 to POE35,000 and PET need to be addressed next.

To explain these differences, one has to note that POE1500 is not a true macromolecule. According to Staudinger, macromolecules should have a molar mass of at least 10 000 Da.³⁰ It also does not reach the entanglement limit for POE of about 8000 Da. The initial sample was crystallized at 300 K. Under these poor crystallization conditions one should have incomplete eutectic separation of the different molecular lengths. On slow, modulated cooling, better crystals result, as is shown in Figure 6, and the maximum in the reversing heat capacity disappears (see Figure 4). An inspection of the Lissajous figures of Figure 9 shows no indication of loss of steady state, assuring that the effect seen for POE1500 is not due to heat-flow limitation or temperature-control problems. From solubility studies of polyethylene with a broad molecular mass distribution after partial melting, it could be shown that on the low-temperature side a melting peak is dominated by the melting of low-molar-mass molecules.³¹ The peak in the apparent, reversing heat capacity of POE1500 on the low-temperature side of the melting peak of Figure 1 points to involvement of low molar mass fractions rather than a local melting–crystallization equilibrium of partially crystallized molecules. Because of the low molar mass of POE1500, there should be no molecules that are anchored in two crystals of different melting points.

The following may be the sequence of events that leads to the reversing apparent heat capacity. When the poor crystals of lowest molar mass melt, the low-temperature cycle may not have exceeded the narrow region of metastability for low molar mass POE, permitting renewed crystallization. This leads again to poor crystals which do not have sufficient time to perfect during the heating portion of the cycle; rather they melt again at the low temperature corresponding to limited crystal perfection. This allows recrystallization on the next cooling cycle. The peak in the reversing heat capacity is thus due to formation and melting of poor crystals. The lower melting temperature of the poor crystals narrows the range of metastability. On better crystallization, the gap between crystal melting and crystallization is too big to be covered by the modulation range, as shown by the second heating in Figure 4. To understand the increase of apparent heat capacity with time shown in Figure 7, one must consider that, after the initial 2 K temperature rise to the new T_0 , all

reversing melting of the previous temperature level stops. A new equilibrium must then develop by diffusion of the proper molar-mass fractions to the surfaces of the remaining crystals. Because of the crystallization cycle, diffusion of the crystallizing species away from the crystals is hindered and, in time, a steady state is established that shows a higher level of reversible melting and crystallization than in the beginning. This multistep mechanism is in need of further confirmation, but TMDSC seems to be able to give the needed experimental information by a combination of changes of modulation parameters and well-characterized molecules and crystals.³² Work in this direction is in progress, making use of homologous series of paraffins.³³

Acknowledgment. This work was financially supported by the Division of Materials Research, NSF, Polymers Program, Grant No. DMR 90-00520 and Oak Ridge National Laboratory, managed by Lockheed Martin Energy Research Corp. for the U.S. Department of Energy, under Contract No. DE-AC05-96OR22464. Support for instrumentation came from TA Instruments, Inc. Research support was also given by ICI Paints and Toray Industries, Inc.

References and Notes

- (1) Wunderlich, B. *Macromolecular Physics; Vol. 2, Crystal Nucleation, Growth, Annealing; Vol. 3, Crystal Melting*; Academic Press: New York, 1976, 1980.
- (2) Ubbelohde, A. R. *Melting and Crystal Structure*; Clarendon Press: Oxford, U.K., 1965.
- (3) Okazaki, I.; Wunderlich, B. *Macromol. Chem., Rapid Commun.*, to be published.
- (4) Okazaki, I.; Wunderlich, B. *Macromolecules* **1997**, *30*, 1758.
- (5) Mehta, A.; Wunderlich, B. *Colloid Polym. Sci.* **1975**, *253*, 193.
- (6) Wunderlich, B.; Mehta, A. *J. Polym. Sci., Polym. Phys. Ed.* **1974**, *12*, 255.
- (7) Wunderlich, B. *Discuss. Faraday. Soc.* **1979**, *68*, 239.
- (8) Blundell, D. J.; Keller, A.; Kovacs, A. *J. Polym. Sci., Part B* **1966**, *4*, 481.
- (9) Frank, F. C.; Keller, A.; Mackley, M. R. *Polymer* **1971**, *12*, 467.
- (10) Reading, M.; Elliot, D.; Hill, V. L. *J. Thermal Anal.* **1993**, *40*, 949.
- (11) Gill, P. S.; Sauerbrunn, S. R.; Reading, M. *J. Thermal Anal.* **1993**, *40*, 931.
- (12) Reading, M. *Trends Polym. Sci.* **1993**, *8*, 248.
- (13) Kovacs, A. J.; Gonthier, A.; Straupe, C. *J. Polym. Sci., Polym. Symp.* **1977**, *50*, 283.
- (14) Kovacs, A. J.; Straupe, C. J.; Gonthier, A. *J. Polym. Sci., Polym. Symp.* **1980**, *59*, 31.
- (15) Cheng, S. Z. D.; Wunderlich, B. *J. Polym. Sci., Part B: Polym. Phys.* **1986**, *24*, 577, 595; *Macromolecules* **1989**, *22*, 1866.
- (16) Boller, A.; Jin, Y.; Wunderlich, B. *J. Thermal Anal.* **1994**, *42*, 307.
- (17) Wunderlich, B.; Jin, Y.; Boller, A. *Thermochim. Acta* **1994**, *238*, 277.
- (18) Wunderlich, B.; Boller, A.; Okazaki, I.; Kreitmeier, S. *Thermochim. Acta* **1996**, *282/83*, 143.
- (19) See WWW (Internet), URL: <http://funnelweb.utcc.utk.edu/~athas>. For a general description, see also: Wunderlich, B. *Pure Appl. Chem.* **1995**, *67*, 1919.
- (20) Zero-entropy-production melting refers either to equilibrium melting or to melting of a metastable crystal to a melt of identical metastability. First proposed for the description of polymer melting by: Wunderlich, B. *Polymer* **1964**, *5*, 611.
- (21) Ditmars, D. A.; Ishihara, S.; Chang, S. S.; Bernstein, G.; West, E. D. *J. Res. Natl. Bur. Stand.* **1982**, *87*, 159.
- (22) Boller, A.; Okazaki, I.; Ishikiriya, K.; Zhang, G.; Wunderlich, B. *J. Thermal Anal.* **1997**, to be published.
- (23) Ishikiriya, K.; Boller, A.; Wunderlich, B. *J. Thermal Anal.* **1997**, to be published.
- (24) Wunderlich, B. *J. Thermal Anal.* **1997**, *48*, 207.
- (25) Okazaki, I.; Wunderlich, B. *J. Polym. Sci., Part B: Polym. Phys.* **1996**, *34*, 2941.
- (26) Boller, A.; Schick, C.; Wunderlich, B. *Thermochim. Acta* **1995**, *266*, 97.
- (27) Van Assche, A.; Van Hemelrijck, A.; Rahier, H.; Van Mele, B. *Thermochim. Acta* **1995**, *268*, 121.
- (28) Toda, A.; Oda, T.; Hikosaka, M.; Daruyama, Y. *Thermochim. Acta* **1997**, to be published.
- (29) Wunderlich, B.; Cormier, C. M. *J. Phys. Chem.* **1966**, *70*, 1844.
- (30) See, for example: Staudinger, H. *Organische Kolloidchemie*, 3rd ed.; Vieweg Verlag: Braunschweig, Germany, 1950.
- (31) Mehta, A.; Wunderlich, B. *Makromol. Chem.* **1974**, *175*, 977.
- (32) Ishikiriya, K.; Wunderlich, B. *J. Polym. Sci., Part B: Polym. Phys.* **1997**, to be published.
- (33) Boller, A.; Ribeiro, M.; Wunderlich, B., to be submitted.

MA961795Q